In the derivation of (9), we have assumed that $K=K'-j0$ for simplicity, so that $\gamma_{+}-\gamma_{-}$ will become infinite at resonance. Also, we have assumed that δ is small enough that $\sin 2\pi x/L$, which occurs in the $h_x h_x^* - h_x^* h_y$ expression, can be replaced by 1 inside the integral, *i.e.*, by setting $x=L/4$ so as to locate the ferrite at the plane of maximum differential propagation.

Further Discussion

From Fig. 3, we observe that the ellipticity for the $c/L=0.15$ case is nearly equal to 1.2, over half of the air-filled region of the waveguide. Thus, a thin slab of ferrite with a width of $x/L \simeq 0.2$ may be placed against the top wall of the waveguide, and adjacent to the dielectric, to obtain good isolation-to-loss ratio or large differential phase shift with low loss over a broad band of frequencies. This configuration has the advantage of higher power-carrying capacity than that of Fig. 1(a). If more isolation or differential phase shift per unit length is desired, two or four ferrite slabs may be placed against the top and/or bottom guide walls on either side of the dielectric slab. In this case, the ferrite slabs on the opposite sides of the dielectric should be oppositely magnetized.

When $\omega < |\gamma_e| (H_a + M_s)$, where H_a is the anisotropy field, low field losses may occur when the ferrite is not saturated. Thus, in the design of tapered-field devices, care should be taken so that the ferrite is saturated at all points, if low field losses would otherwise occur. If the dc magnetic-field configuration is such that this cannot be achieved, it would be best to eliminate the unsaturated portion or to replace that portion by a dielectric of about the same dielectric constant.

Theory of TEM Diode Switching*

ROBERT V. GARVER†, MEMBER, IRE

Summary—**The theory of TEM diode switching is presented for the purpose of understanding and designing TEM microwave diode switches. A few experimental results are reported for the purpose of supporting the theory and demonstrating the exceptional bandwidth possible.**

An analysis is given of the switching action of one and of two or more diodes as well as the biasing of the center conductor of a TEM transmission line over broad-frequency bandwidths without interacting with the RF signal. The use of point-contact germanium, varactor, and gold-bonded germanium diodes for TEM switching is discussed. Some considerations of switching speed and maximum power-handling capacity are given.

A coaxial transmission line switch has been constructed in which two gold-bonded diodes provide 26-db or greater isolation and insertion loss ranging from 1.6 db to less than 1 db from 40 Mc to 4000 Mc. The addition of a bias lead should increase the insertion loss 0.4 db or less over the 100-to-1 bandwidth, the maximum increase being at the upper and lower bounds.

I. Introduction

For some years a technique for switching microwaves in X-band waveguide with semiconductor diodes has been in use [1]. Attempts to understand this switching action led to a theory of semiconductor diode microwave switching by use of point-contact germanium diodes [2]. Other investigators found a more direct theory for isolation [3] and proved the good possibilities of using varactor diodes [4] and gold-bonded diodes [5] in coaxial transmission lines for switching. This report covers a more thorough investigation of the theory of TEM microwave diode switching and presents some modes of operation heretofore unreported.

When discussing diode switching it is necessary to define certain terms. RF power incident on an ideal attenuating device is either absorbed in or transmitted past the device, with no power reflected. The attenuation α of the device is defined as the ratio in decibels of the incident power to the transmitted power. If the attenuation of the device can be changed from some low value to some high value the device is called a switch. The insertion loss δ is defined as the minimum attenuation, and the isolation η is defined as the maximum attenuation.

When a diode is inserted in series or in shunt in a transmission line, RF power incident on the diode is reflected by, absorbed in, or transmitted past the diode. A diode is different from an attenuating device in that most of the incident RF power not transmitted is reflected rather than absorbed. In fact, in an ideal diode switch, the incident power is either completely reflected or completely transmitted. The definitions of attenuation, insertion loss, and isolation are the same for a diode switch as for an absorption switch.

* Received by the PGMTT, September 20, 1960.
† Diamond Ordnance Fuze Laboratories, Washington 25, D. C.

II. Basic Concepts

To obtain attenuation by use of a single diode element in a TEM wave transmission line, the diode is mounted either in series with the center conductor or in shunt across the center and outer conductors. The derivation of attenuation will be briefly reviewed. For a more thorough treatment see Riebman [3].

The RF power transmitted past the diode is, in all cases, the power delivered to the matched load. The incident RF power must be visualized as the forward traveling wave incident on the diode, considered for the moment to be in a holder which is a four-terminal transmission line device [6]. For the purpose of deriving the attenuation resulting from diode impedance and admittance, the diode is visualized as a two-terminal device whose RF impedance can be varied by changing the applied voltage. The equivalent circuits are shown in Fig. 1. If the diode is considered to be of zero thickness and in a bilaterally matched transmission line, then the equivalent circuits are valid for most calculations.

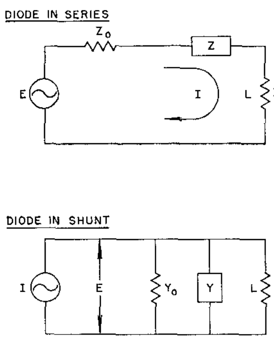

Fig. 1—The equivalent circuits of a diode impedance Z in series and admittance Y in shunt in a transmission line.

In the equivalent circuit of a series-connected diode (Fig. 1), E is the peak amplitude of the sinusoidal voltage source which is assumed to have an output impedance Z_0; Z represents the diode, and $L(=Z_0)$ is the matched load behind it. I is the peak amplitude of the resulting sinusoidal current. The power P_L in L is given by

$$P_L = \tfrac{1}{2} II^* Z_0. \tag{1}$$

If $Z=R+jX$ then the power P_T transmitted to the load is given by

$$P_T = \frac{1}{2}\,\frac{E^2 Z_0}{(R+2Z_0)^2+X^2}\,. \tag{2}$$

The power P_i incident on the diode is the power in the forward traveling wave going toward L. This is attained in the series equivalent circuit by setting Z equal to zero. So

$$P_i = \frac{E^2}{8Z_0} \tag{3}$$

and the resulting attenuation is

$$\alpha = 10\log\frac{P_i}{P_T} = 10\log\frac{\left(\frac{R}{Z_0}+2\right)^2+\left(\frac{X}{Z_0}\right)^2}{4}\,. \tag{4}$$

For a diode in shunt having an admittance $Y=G+jB$, the derivation of attenuation is the same as above with the substitution of Y for Z, I for E, etc. Thus,

$$P_L = \tfrac{1}{2} EE^* Y_0 \tag{5}$$

and

$$\alpha = 10\log\frac{\left(\frac{G}{Y_0}+2\right)^2+\left(\frac{B}{Y_0}\right)^2}{4}\,. \tag{6}$$

Equi-attenuation curves are circular arcs on a rectangular grid plot of normalized impedance or admittance with their centers at $-2+j0$ and radii of $2\times10^{\alpha/20}$, or circular arcs on the Smith Chart as shown in Fig. 2.

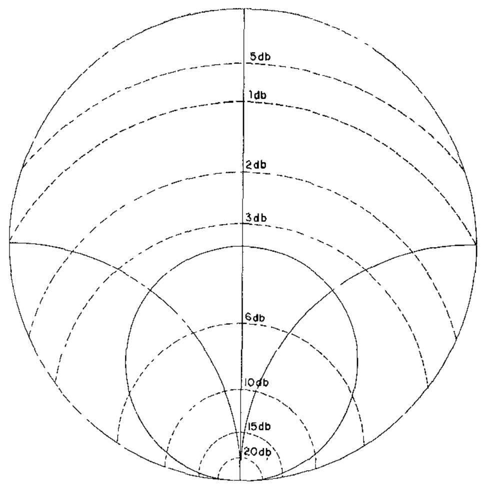

Fig. 2—Smith Chart plot of equal attenuation curves.

The diodes most suited for switching at high frequencies are the point-contact germanium, gold-bonded, and varactor diodes by virtue of their low spreading resistance (R_s) at forward bias and small depletion layer capacitance (C_d) at reverse bias (Fig. 3). In the fabrication of these diodes use is made of a fine wire, or whisker, that makes contact with the active region of the diode. The whisker and semiconductor are each attached to pieces of metal that are supported by a ceramic or glass tube, and to which the diode connecting leads are attached. This whisker introduces a small but not negligible series inductance (L_W). An appreciable capacitance exists between these metal end pieces, denoted as the cartridge capacitance C_c in Fig. 3. This capacitance is 0.16 pf for the 1N23 and 1N263 microwave cartridges, and is much less for the glass cartridge used with gold-bonded diodes. L_w varies from 2 to 10 nh depending on the length and diameter of the whisker. C_d ranges from 0.05 to 0.2 pf, some good gold-bonded diodes giving 0.2 pf and the best varactors giving 0.05 pf. For point-contact germanium diodes, C_d varies from 0.2 pf at low frequencies to 0.015 pf at UHF. In available diodes, R_s ranges from 3 ohms for gold-bonded diodes to 10 ohms for varactors and point-contact germanium diodes. The reactance of these parameters in the frequency range of interest is plotted in the reactance frequency chart of Fig. 4.

At forward bias, the equivalent circuit (Fig. 3) is valid for all three types of diodes. At reverse bias, the equivalent circuit is valid for varactors and gold-bonded diodes, but is invalid for point-contact germanium diodes because C_d has a resistance in parallel with it which is about 5000 ohms [2].

In Fig. 5, the attenuation from a diode shunting a 50-ohm transmission line is plotted as a function of diode impedance. The R_s of forward-biased diodes will allow 10- to 20-db isolation at frequencies below 200 Mc, since the reactance of L_w will generally be less than 5 ohms below this frequency.

At reverse bias, the capacitance C_c+C_d is the dominant impedance. The insertion loss for $C_c+C_d=0.2$ pf is less than 0.1 db for all frequencies below 5 Gc. Note from Fig. 5 that if $R_s=50$ ohms and $L_w=2$ nh, which may be found in a gold-bonded diode, it is possible to have a constant isolation of 3 db with a very low insertion loss for all frequencies up to that corresponding to $2\pi f L_w=30$ ohms, which is 2 Gc. A very flat, low-insertion loss, 3-db modulator is then possible. Other values of isolation are possible by selecting the proper R_s.

For a diode in series in a 50-ohm transmission line the attenuation is depicted in Fig. 6 as a function of the diode impedance. The diode impedances at forward bias for frequencies below 2 Gc result in insertion loss in the 1-db region. In conjunction with Fig. 4, Fig. 6 reveals that a capacitance C_d+C_c of 0.2 pf results in isolation of approximately 20 db up to about 1 Gc. Figs. 5 and 6 in conjunction with Fig. 4 are useful for quickly determining the frequency range and basic configuration in which a diode can be made to switch. From these figures it is apparent that the available diodes give greater isolation at higher frequencies without considerable sacrifice in insertion loss when used in the series configuration in a 50-ohm TEM transmission line. In general, if the diode impedance is variable from $1/20Z_0$ to $4Z_0$, the shunt configuration is indicated; and if the diode impedance is variable from $1/4Z_0$ to $20Z_0$,

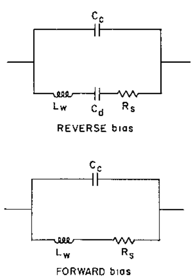

TYPICAL VALUES

	POINT CONTACT GER DIODES	GOLD BONDED DIODES	VARACTOR DIODES
R_s—Ω	6	4	10-2
L_w—nh	5	2	5
C_d—pf	015	2	2-.05
C_c—pf	16	05	16

Fig. 3—Equivalent circuits of a diode at reverse bias and forward bias.

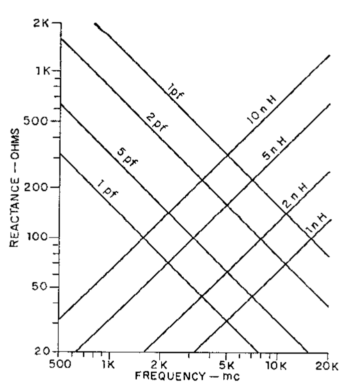

Fig. 4—Enlarged reactance-frequency plot.

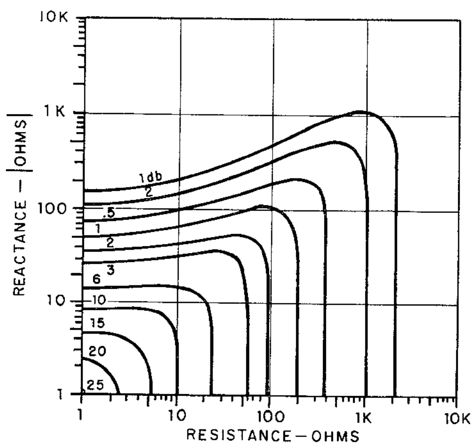

Fig. 5—Attenuation resulting from a diode shunting 50-ohm transmission line as a function of diode impedance.

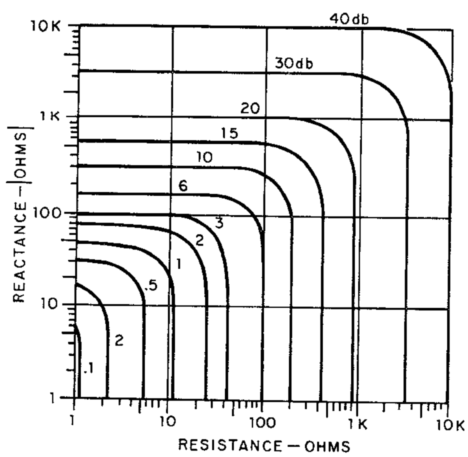

Fig. 6—Attenuation resulting from a diode in series in 50-ohm transmission line as a function of diode impedance.

the series configuration is indicated. Note also that switching improves as frequency decreases, indicating broad-band switching down to any desired frequency.

III. Diode Modes

A. Series Diode

As a function of frequency, the computed attenuation of a series diode in a 50-ohm transmission line is shown in Fig. 7. The equivalent circuit parameters shown in Fig. 3 are $C_c=0.2$ pf, $L_w=5$ nh, $C_d=0.2$ pf, and $R_s=5$ ohms. It is assumed that these parameters do not change drastically with frequency. From Fig. 7 it is seen that high isolation is available at three frequencies, which are labeled Modes 1, 2, and 3. In Mode 1, the insertion loss is low, as previously discussed. The isolation of Mode 2 is the result of parallel resonance between C_c and L_w at forward bias, and the insertion loss is the result of a series resonance between L_w and C_d at reverse bias. By picking $C_c=C_d$, these resonances are made to occur at the same frequency so that Mode 2 has a low insertion loss. Mode 3 is caused by the reverse bias parallel resonance between C_c and L_w in combination with C_d.

1) Mode 1: Expanded curves for Mode 1 are shown in Fig. 8. Here it is assumed for the C_c+C_d curves that the diode is at reverse bias and $R_s=L_w=0$. For the L_w curves it is assumed that the diode is at forward bias and $C_c=0$ and $R_s=5$ ohms. One sees that the combination of $C_c+C_d=0.2$ pf and $L_w=5$ nh allows for 10 db or greater switching up to 2 Gc. It is also seen how with a given C_c+C_d the isolation increases with decreasing frequency. This increase continues until the reactance of C_c+C_d becomes greater than the depletion region resistance, at which point the resistance becomes the predominant factor in determining the isolation.

With Mode 1 operation, the insertion loss becomes undesirably large at higher frequencies due to L_w; at 2 Gc, 5 nh already results in 2-db insertion loss. Another effect of L_w is to decrease isolation slightly by lowering the reactance presented by C_c+C_d. Because the whisker is of nonzero length it can be more accurately described as a short length of high-impedance TEM-wave transmission line, and the effect of L_w will be slightly less than depicted in Fig. 8.

A method of decreasing the effect of L_w is to increase the distributed capacitance from the inner conductor to the outer conductor in the region of the diode, thus maintaining $Z_0=\sqrt{L/C}=50$ ohms. A technique for attaining this without greatly increasing C_c is shown in Fig. 9. The length of the abrupt 50-ohm tapers is controlled to provide the desired amount of shunt capacitance.

2) Mode 2: Mode 2 will normally exist for most diodes, but the maximum isolation and minimum insertion loss may not occur at the same frequency. To cause them to occur at the same frequency, C_c can be increased as illustrated in Fig. 10 so that $C_c=C_d$. To reduce the frequency of the maximum isolation, it is necessary to apply less than maximum reverse bias which increases C_d. To increase this frequency it is necessary to decrease L_w. Riebman [4] found Mode 2 to be useful between 8 and 12 Gc.

3) Mode 3: As seen from Fig. 7, Mode 3 has an associated high insertion loss. One method of decreasing the insertion loss is to increase the separation between Modes 2 and 3. When this is done by increasing C_c, both modes move down in frequency as the separation increases and the maximum isolation of Mode 3 decreases. Attempts to increase the operating frequency of Mode 3 result in a decrease of separation between Modes 2 and 3, plus a higher insertion loss for Mode 3. A more suitable method for decreasing the insertion loss is to place an inductor in series with the diode. The diode at forward bias at Mode 3 is capacitive, and a series resonance results in reduced insertion loss. The series inductance may be a short length of high-impedance transmission line immediately adjacent to the diode.

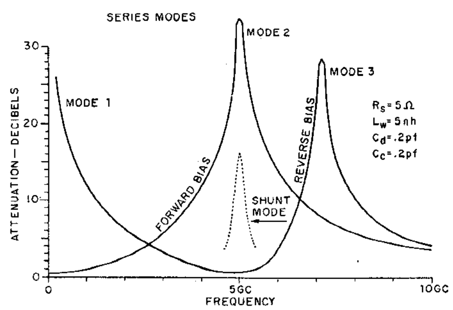

Fig. 7—Switching modes of a diode in series in 50-ohm transmission line.

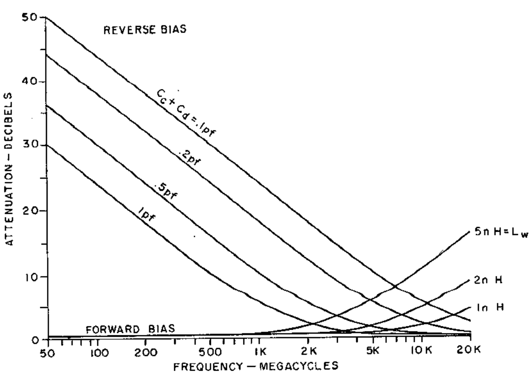

Fig. 8—Detailed presentation of Mode 1 operation. For the "C_c+C_d" curves it is assumed that the diode is at reverse bias and that $R_s=L_w=0$. For the "L_w" curves it is assumed that $C_c=0$ and $R_s=5$ ohms. These same curves describe the bandwidth of the isolation and insertion loss of the diode operating in the other series modes.

B. Shunt Diode

Fig. 11 shows the computed attenuation of a shunt diode in a 50-ohm transmission line as a function of frequency. The diode equivalent circuit parameters are the same as those picked for the series diode of Fig.

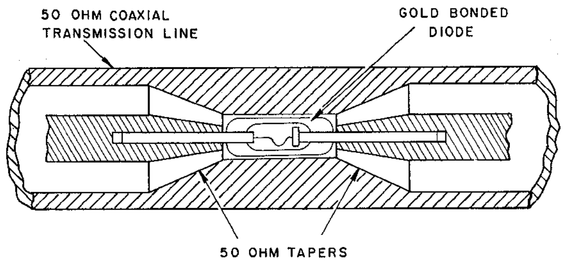

Fig. 9—Phantom view of a diode in a configuration for increasing the capacitance to the outside conductor (without increasing C_c) to reduce the effect of L_w.

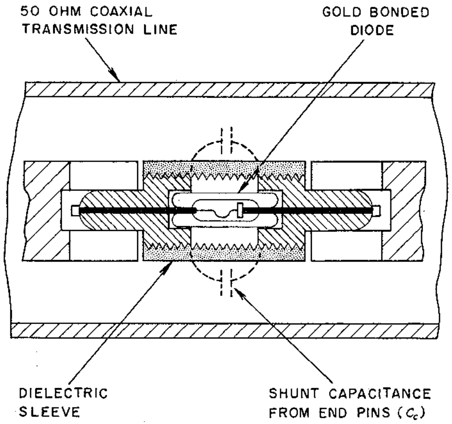

Fig. 10—Phantom view of a diode in a configuration for controlling Mode 2 operation by increased cartridge shunt capacitance.

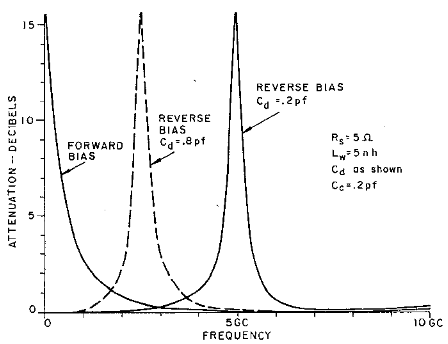

Fig. 11—Switching modes of a diode shunting 50-ohm transmission line.

7. At forward bias, high isolation occurs only at low frequencies. At reverse bias, high isolation occurs only at the frequency corresponding to the series resonance between L_w and C_d. The insertion losses associated with the low and high isolation frequencies are very low because of the high reactances of C_c+C_d, and L_w, respectively. A curve for the resonant shunt mode is also given in Fig. 7 for comparison with the curve for series Mode 2 with respect to bandwidth and maximum isolation.

A very efficient switch can be made using a varactor as a shunt diode. If it is assumed that the varactor capacitance C_d can increase to 0.8 pf before conduction starts, then the resonant shunt mode will appear as shown by the dashed curve in Fig. 11. The switch behaves as a voltage-tunable, band-rejection filter, drawing practically no current and able to cause switching at any frequency in its tunable range. At the two frequencies shown, 2.5 and 5 Gc, the attenuation can be varied from 15 db to less than 0.2 db. Section V below will show that the use of more than one diode will increase the isolation and bandwidth beyond that attainable with a single diode. The frequency range of this configuration can be further controlled by placing additional inductance in series with the diode. The insertion loss resulting from C_c can be decreased by making the center conductor diameter smaller, which increases the coaxial line inductance per unit length, keeping $Z_0=\sqrt{L/C}=50$ ohms constant. This configuration provides a very efficient switch for low-power microwaves since the switching occurs entirely at reverse bias, drawing essentially no current.

C. A Modified Series Mode

1) Mode $1\frac{1}{2}$: Riebman [4] has developed a technique for extending the range of Mode 1-type operation by placing an inductor L_T in parallel with C_c+C_d to resonate with their reactance and restore high isolation. This technique will be called Mode $1\frac{1}{2}$ operation. Here the technique of reducing the effect of L_w is useful to maintain low forward bias insertion loss at these higher frequencies. The equivalent circuit for Mode $1\frac{1}{2}$ operation is shown in Fig. 12. L_T is the inductor used in tuning C_c+C_d to the desired operating frequency range. C_b prevents L_T from shunting out the dc switching voltage. It was shown by Riebman [4] that the design frequency should be the geometric mean of the minimum and maximum frequencies of the desired operating range. The isolation is then equal at the extremes. A Mode $1\frac{1}{2}$ diode switch can be fabricated easily by wrapping eight turns of fine enameled wire around the 1N263 glass tube with several closely packed tight turns around the pin ends of the diode. The insulation is left on the fine wire to provide C_b at the ends. The wire can then be anchored with Q dope. Such a configuration will be optimum at about 1 Gc. Based upon C_d+C_c of 0.2 pf, calculated isolations for Mode $1\frac{1}{2}$ are shown in Fig. 13 for several design frequencies. Average isolation values for two AEL Model CM/2/4 diode switches are shown as the plotted points in Fig. 13. The operation can be shifted down in frequency by applying less than maximum reverse bias voltage on the diodes. (Note that for a given isolation, the bandwidth in Mc remains constant for a given C_d+C_c rather than the ratio of upper frequency to the lower frequency remaining constant.) The bandwidth and maximum isolation at the resonant frequency are given in Section IV. The bandwidth is exactly the bandwidth of Mode 1 which is plotted in Fig. 8. It is seen that for lower C_d+C_c greater bandwidth is possible. Lowering the operating frequency by reducing the reverse bias thus reduces the bandwidth as well. For lower frequency operation of Mode $1\frac{1}{2}$, a resonance between L_T and

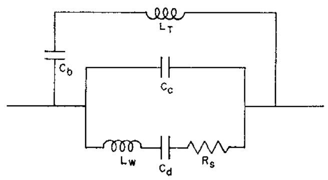

Fig. 12—Equivalent circuit for Mode $1\frac{1}{2}$ operation.

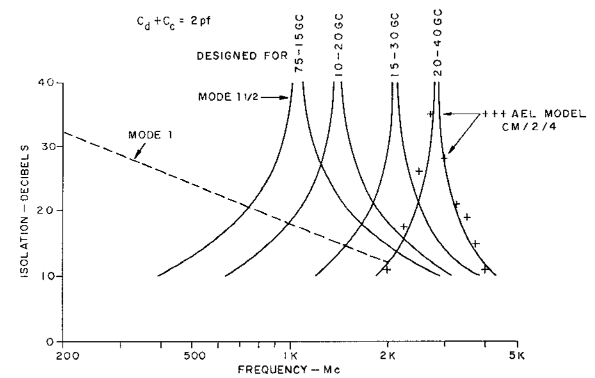

Fig. 13—Isolation for Mode $1\frac{1}{2}$ switching for various tunings.

C_b must be avoided by making C_b large. The construction used in the CM/2/4 attains this as well as being rugged. The Mode 1 curve for $C_d+C_c=0.2$ pf is given in Fig. 13 to show the improvement at higher frequencies afforded by Mode $1\frac{1}{2}$.

IV. Bandwidth

A. *Isolation*

The isolation of a series diode switch results from the high reactive impedance of the diode. In a 50-ohm transmission line, when $R/Z_0 \ll 1$ and $X/Z_0 \geq 6$, the isolation given by (4) reduces to

$$\eta \approx 20 \log \frac{|X|}{100} \tag{7}$$

with an error of less than 5 per cent. This relation is valid for isolation greater than 10 db and frequencies slightly away from any resonances. Thus, for a specified isolation, the required series reactance is

$$|X| = 100 \times 10^{\eta/20}. \tag{8}$$

If X is due to a parallel combination of L and C (such as L_T and C_c+C_d in Fig. 12), the susceptance of the pair is

$$\frac{1}{X} = 2\pi f C - \frac{1}{2\pi f L} \cdot \tag{9}$$

Solving for f:

$$f = \frac{1}{4\pi C X} + \frac{1}{2\pi}\sqrt{\frac{1}{4C^2X^2} + \frac{1}{LC}} \cdot \tag{10}$$

Given a value of X, the isolation will increase as the parallel resonant frequency is approached and then decrease to the same isolation as $-X$ is approached. The bandwidth is the difference between the frequencies that correspond to X and $-X$. Over the bandwidth, the isolation is maximum at parallel resonance and minimum at the extremes which correspond to X and $-X$. Substituting $-X$ for X in (10) and then subtracting from the same, the bandwidth is obtained:

$$\Delta f = f(X) - f(-X) = \frac{1}{2\pi C|X|} = [200\pi C \times 10^{\eta/20}]^{-1}. \tag{11}$$

Note that L does not appear in the equation and that the isolation bandwidth is a function of specified isolation and C (and Z_0) only.

For Mode 1, L is assumed to be infinite. The isolation results from a capacitor alone in series in the transmission line. Thus Fig. 8 shows not only an extended plot of Mode 1 operation, but also shows the plot of isolation bandwidth, (11).

The resonance causing Mode 2 isolation is between C_c and L_w (Fig. 3). In this case C_c rather than C_c+C_d determines the bandwidth. If $C_c=C_d$, Mode 2 bandwidth is twice that of Mode 1 (Fig. 7).

Mode 3 is the result of a series-parallel antiresonance of C_c, L_w, and C_d, which occurs at $\sqrt{2}$ times the center frequency of Mode 2 when $C_c=C_d$ and has the same bandwidth as Mode 1.

Mode $1\frac{1}{2}$ (Fig. 13) is a resonance between L_T and C_c+C_d; thus, the bandwidth is determined by C_c+C_d. The Mode $1\frac{1}{2}$ technique can be visualized as simply causing Mode 1 operation to be shifted to higher frequencies, since their bandwidths are exactly the same.

At and near the parallel resonance between L and C, the isolation is limited by any R in series with L or C. At resonance, the impedance of the diode is $Z \approx X^2/R + j0$ where X is the reactance of the L or C in series with R. The isolation from this impedance in a 50-ohm transmission line is

$$\eta \approx 20 \log \frac{X^2}{100R} \cdot \tag{12}$$

For Mode $1\frac{1}{2}$, C_d is in series with R_s. For Mode 2, L_w is in series with R_s. For Mode 3, the inductive reactance of the L_w, C_d combination is in series with R_s; and at resonance, their reactance is equal to that of C_c.

The bandwidth of a diode switch shunting the transmission line is similar in derivation to that of the series diode. The isolation results from the low impedance of a series resonance between an L and a C. Isolations above 10 db in a 50-ohm transmission line are given approximately by

$$\eta = 20 \log \left(\frac{25}{|X|}\right), \tag{13}$$

where X is the shunting reactance.

Solving for $|X|$:

$$|X| = 25 \times 10^{-\eta/20}. \tag{14}$$

The reactance of the shunting series LC is

$$X = 2\pi fL - \frac{1}{2\pi fC} \cdot \quad (15)$$

Solving for f,

$$f = \frac{X}{4\pi L} + \frac{1}{2\pi}\sqrt{\frac{X^2}{4L^2} + \frac{1}{LC}} \cdot \quad (16)$$

Substituting $-X$ for X as before, and subtracting:

$$\Delta f = f(X) - f(-X) = \frac{|X|}{2\pi L} = \frac{25}{2\pi L} \times 10^{-\eta/20}. \quad (17)$$

It is seen here that the bandwidth is dependent only on L and η (and Z_0).

Comparison is made between the bandwidths of series and shunt switches at the 20-db points. They are, respectively, $1/2000\pi C$ and $25/20\pi L$. Assuming R_s is low enough to allow good shunt switching, L must be no larger than $2500C$ for equal bandwidths. A capacitance of 0.2 pf is readily available. For an equal bandwidth, then, an inductance of 0.5 nh is needed. Such a small inductance is obtainable in pill-type diode cartridges designed for stripline applications. With a whisker inductance of 2 nh, the bandwidth of the shunt switch is only one fourth that of the series switch. If the frequency of the resonant shunt mode is lowered by increasing the series inductance, the bandwidth is decreased. Electrically tuning the resonant shunt mode as in Fig. 11 does not alter the bandwidth.

B. Insertion Loss

The insertion loss of a series diode switch results either from the low impedance of R_s and L_w for Mode 1, or a series resonance between C_d and L_w for Mode 2.

$$Z = R_s + j\left(2\pi fL_w - \frac{1}{2\pi fC_d}\right) = R_s + jX. \quad (18)$$

From Section II, the insertion loss in a 50-ohm transmission line is given by the relation

$$\delta = 10 \log\left[\left(1 + \frac{R_s}{100}\right)^2 + \left(\frac{X}{100}\right)^2\right]. \quad (19)$$

Solving for X:

$$|X| = 100\left[10^{\delta/10} - \left(1 + \frac{R_s}{100}\right)^2\right]^{1/2}. \quad (20)$$

Solving for the bandwidth as before:

$$\Delta f = \frac{|X|}{2\pi L_w} = \frac{50}{\pi L_w}\left[10^{\delta/10} - \left(1 + \frac{R_s}{100}\right)^2\right]^{1/2}. \quad (21)$$

The insertion-loss bandwidth is not a function of C_d and is also plotted in Fig. 8.

The insertion loss of a shunting diode in the frequency range of interest (Fig. 11) is less than some maximum value δ from zero to a maximum frequency $f_{\max}$ at reverse bias; at forward bias it is below δ for frequencies above a minimum frequency $f_{\min}$. The insertion loss of a shunting diode comes from low susceptance and negligible conductance. From (6):

$$\delta = 10 \log\left[1 + \left(\frac{B}{2Y_0}\right)^2\right] \approx 4.35\left(\frac{B}{2Y_0}\right)^2 \quad (22)$$

for a small insertion loss.

Solving for B in a 50-ohm transmission line:

$$B = \frac{\sqrt{\delta}}{52} \cdot \quad (23)$$

At reverse bias:

$$B = 2\pi fC, \quad \text{and} \quad f_{\max} = \frac{\sqrt{\delta}}{327C} \cdot \quad (24)$$

The insertion loss is less than δ up to $f_{\max}$. At forward bias:

$$B = \frac{1}{2\pi fL_w} \quad (25)$$

and

$$f_{\min} = \frac{1}{2\pi BL_w} = \frac{8.28}{\sqrt{\delta}\, L_w} \cdot \quad (26)$$

The insertion loss is less than δ above $f_{\min}$. If a resonant shunt diode switch is to be made by using pill-type diodes in stripline, C_c may have to be increased to cause the insertion loss to be reduced at the switching frequency.

C. Diode Quality Factor, f_c

The bandwidth of the series diode switch (Mode 1) for given values of isolation η and insertion loss δ can be derived in terms of the diode quality factor, or the so-called cut-off frequency f_c.

$$f_c = \frac{1}{2\pi CR_s} \cdot \quad (27)$$

From (11), the derived expression for bandwidth is

$$\begin{aligned}\Delta f &= [200\pi C \times 10^{\eta/20}]^{-1} \\ &= [(2\pi C)(2Z_0 \times 10^{\eta/20})]^{-1} \\ &= f_c \frac{R_s}{2Z_0} 10^{-\eta/20}. \quad (28)\end{aligned}$$

The insertion loss is usually more broadband than the isolation, and this will be considered to be frequency independent, as expressed by (4);

$$\delta = 20 \log \left(1 + \frac{R_s}{2Z_0}\right)$$
$$\approx 8.7 \frac{R_s}{2Z_0}. \tag{29}$$

Rearranging (29), and substituting into (28), we obtain

$$\Delta f = f_c \frac{\delta}{8.7} 10^{-\eta/20}. \tag{30}$$

A diode of $f_c = 200$ Gc can give 30-db or greater isolation and 0.2-db insertion loss over 147-Mc bandwidth, or it can give 20-db or greater isolation and 0.5-db insertion loss over 1150-Mc bandwidth. The transmission line characteristic impedance Z_0 is varied to give the desired combination.

V. Multiple Switching Elements

Where higher isolation is required than is possible with one diode, two or more diodes may be used [7]. The total isolation from multiple diodes is a function of the spacing between them. At optimum spacing, the total isolation is larger than the sum of individual isolations. For theoretical analysis, the diodes in the isolating state are considered to be equal, lossless reactances. The spacing between two equal reactances for minimum reflected power is a function of their normalized reactance [9]. For maximum reflected power, the spacing l/λ_g is a quarter wavelength different from that for minimum reflection (Appendix I),

$$\frac{l}{\lambda_g} = \frac{1}{4} + \frac{1}{2\pi}\left[\tan^{-1}\frac{2}{X/Z_0}\right]. \tag{31}$$

Eq. 31 is plotted in Fig. 14 as the curve intersecting the l/λ axis at 0 and 0.5. The curve for minimum reflection is shown as the curve intersecting the l/λ axis at 0.25. The relations are the same whether the reflectors are in series or in shunt. The spacing for mismatch is optimum not only for two elements but also for any number of elements. Using the transmission line equation, the attenuation of two equal reactances was calculated as a function of separation and plotted as equi-attenuation curves in Fig. 14. A Mode 1 series diode and a nonresonant mode shunt diode are a negative reactance and susceptance, respectively. For example, assume they are represented by the point at -4 on the maximum reflection curve in Fig. 14. For a maximum isolation at some high frequency, l/λ is made 0.175. As the frequency is decreased, l/λ decreases for a fixed l and the reactance or susceptance increases, causing the plot of the parameters to follow a hyperbola. Following the hyperbola, increasingly higher equi-attenuation curves are intersected, indicating not only improved isolation at the highest frequency but ever increasing attenuation at lower frequencies. The calculated isolation of two elements for a fixed spacing follows closely a curve for a smaller capacitance as in Fig. 8. Thus, the series Mode 1 and the nonresonant shunt mode can be extended up in frequency with no sacrifice in isolation at lower frequencies.

When equal reactive elements are spaced for maximum attenuation, the total attenuation is greater than the sum of individual attenuations. This is termed extra attenuation α_{xn}. In Appendix I, α_{x2} is derived and a simplified calculation for other α_{xn} is described. The extra attenuation for $n = 1$, 2, 3, 4 and ∞ is plotted in Fig. 15. If one diode gives α_1-db attenuation, then the total attenuation α_T of N optimum spaced identical diode is

$$\alpha_T = N\alpha_1 + \sum_{n=1}^{N} \alpha_{xn}. \tag{32}$$

As an example of the use of multiple diodes, suppose it is desired to extend Mode 1 operation to 4 Gc, using two gold-bonded diodes having a $C_c + C_d$ of 0.2 pf, and R_s of 5 ohms, and an L_w that is negligible. At 4 Gc the capacitive reactance is 200 ohms (Fig. 4), which corresponds to an X/Z_0 of -4. Then, according to Fig. 14, the spacing should be 0.175 λ_g. In an air dielectic coaxial line, this spacing is 0.519 inch. Now, by Fig. 8, the isolation with 0.2 pf at 4 Gc is 7 db. By Fig. 15 and (32), the total isolation at 4 Gc is 19.2 db. The isolation

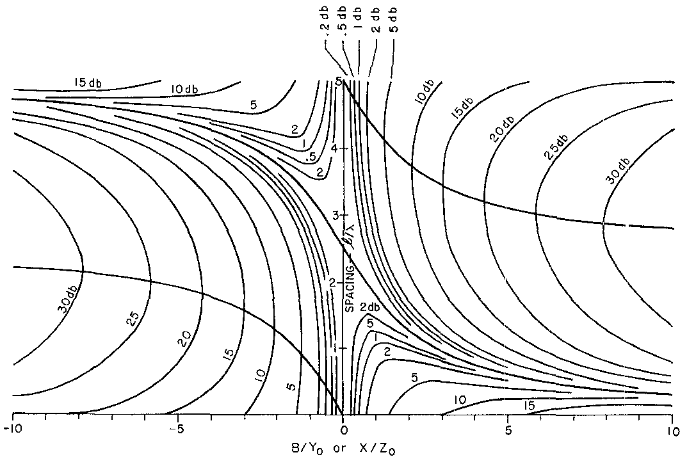

Fig. 14—Attenuation of two equal reactive (or susceptive) elements as a function of their separation and normalized reactance (or susceptance). The curve for match intersects the l/λ axis at 0.25 while the mismatch curves intersect it at 0 and 0.5.

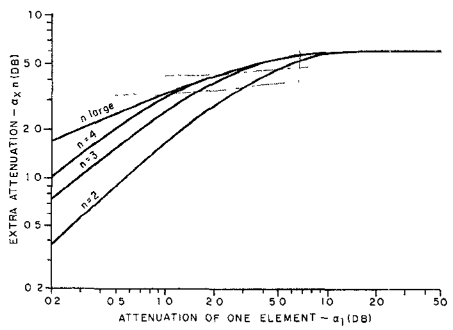

Fig. 15—Extra attenuation resulting from a second, third, and fourth equal element and the limit approached for many equal elements, as a function of the attenuation of one element.

of these two diodes with a fixed spacing was calculated for decreasing frequency and was found to behave approximately as that of $C_e+C_d=0.04$ pf. If L_w is sufficiently small, each diode will have about 0.5-db insertion loss at forward bias. Being nonreactive, the insertion loss adds with no extra attenuation; thus, the insertion loss of two of these diodes should be about one db.

As another example, the calculated isolation of four 0.2-pf diodes at 10 Gc with optimum spacing is 20 db. If L_w is reduced below 0.5 nh, the insertion loss would be about 2 db.

Data from a switch made by using one and two gold-bonded diodes is shown in Fig. 16. Photographs of the switch assembled and unassembled are shown in Fig. 17. For one diode, the insertion loss is less than one db for all frequencies shown, and the isolation is a minimum of 17 db at 4 Gc. For two diodes it was difficult to obtain a low insertion loss at all frequencies. To obtain the insertion loss shown, the spacing for maximum isolation could not be used. The isolation at 4 Gc is 26 db. The insertion loss is a maximum of 1.6 db at two frequencies, and less than one db at other frequencies. It is believed that the design could be improved to more closely approach the theoretical isolation and insertion losses of 40 db and one db, respectively, at 4 Gc.

One might think that if C_b in Fig. 12 can be made large enough for Mode $1\frac{1}{2}$ operation, the use of one Mode 1 diode and one Mode $1\frac{1}{2}$ diode separated by some calculated spacing would give a broad-band switch with better performance at the higher frequencies than is obtained with two Mode 1 diodes. However, below the parallel resonant frequency of the Mode $1\frac{1}{2}$ diode, the diode impedance is inductive, and this would be in series with a capacitive Mode 1 diode. A series resonance would then occur at some lower frequency. Below the resonance, the isolation would be less than that of one Mode 1 diode. For a broad-band switch, this is not desirable. Such a configuration might be useful, however, as a tunable narrow band-pass filter or efficient narrow-band switch. This is to be compared with shunt mode diodes producing tunable narrow-band rejection.

Many combinations of diode modes are possible for a great variety of switching results. It is believed, however, that the most broad-band configuration is obtained by placing Mode 1 diodes in series.

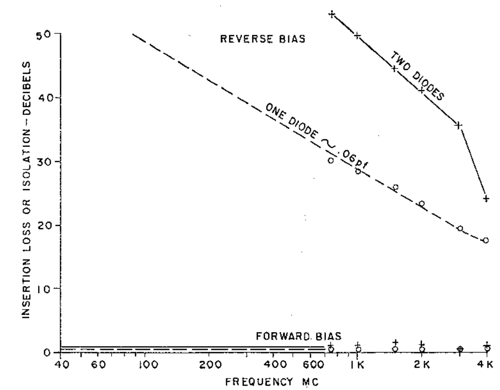

Fig. 16—Experimental characteristics of a 40-Mc to 4-Gc switch using one and two gold-bonded diodes.

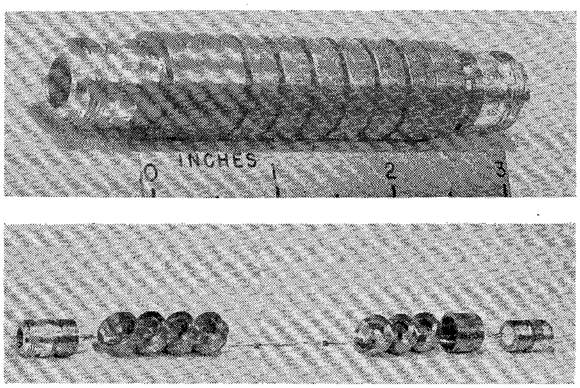

Fig. 17—Photograph of 40-Mc to 4-Gc diode switch.

VI. Biasing Circuitry

To produce switching action with a diode, it is necessary to supply a switching signal to the diode. It is most desirable to have no interaction between the biasing circuitry and the microwave circuitry. For a diode in series or in shunt, all of the components for the needed isolation between circuits are shown in Fig. 18. C_2 and C_3 can be omitted in many applications or they can be built into the end connectors [4]. An 0.0005-inch gap in a center conductor of 0.25-inch diameter has a capacitance of about 20 pf, which results in 1-db insertion loss at 160 Mc and less than 0.1 db above 600 Mc. L_2 and C_3 are not used if a ground return exists in some other component in the line. At the lowest frequency to be used, the reactance of C_1 should be less than one tenth of the impedance of L_1 for the series switch or of the diode for the shunt arrangement.

The diode switching element is broad band. The capacitors just discussed are broad band. The biasing

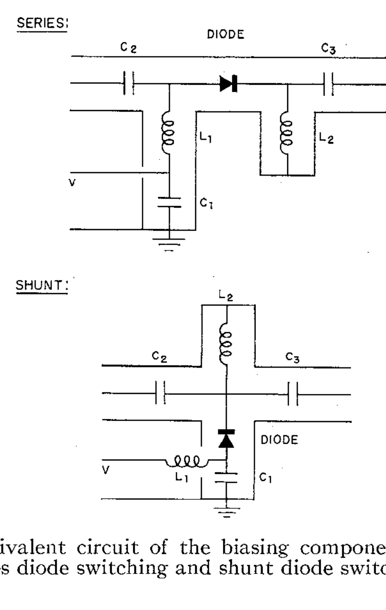

Fig. 18—Equivalent circuit of the biasing components needed for series diode switching and shunt diode switching.

inductors must therefore be made broad band in order to have a broad-band switch. At lower frequencies prewound RF inductors are satisfactory. Since the reactance of an inductor decreases with decreasing frequency, a sufficiently large inductance must be selected for a given minimum operating frequency. For higher frequencies, however, the self-resonance in a large prewound RF inductor may cause trouble. Also, for high-speed switching a large inductor is undesirable. Therefore, another approach to the design of the biasing lead is needed.

In prior designs, the center conductors in coaxial waveguides were supported by shorted quarter wavelength coaxial sections. These supports had little effect on the microwave transmission over considerable bandwidths. By substituting a capacitance for the short and making the characteristic impedance of the quarter-wavelength line section equal to that of the main guide (Z_0), a bias can be applied to this lead with an attenuation of $\frac{1}{4}$ db or less over a 2-to-1 frequency range. Greater bandwidth can be obtained by using shorted quarter-wavelength biasing leads having higher characteristic impedance as shown below.

The impedance of a shorted length of lossless transmission line of characteristic impedance Z_g is

$$Z = jX = jZ_g \tan\left(\frac{2\pi l}{\lambda}\right). \qquad (33)$$

This is plotted in Fig. 19. For a lossless shunting reactance $G/Y_0 = 0$. From (6)

$$\alpha = 10 \log\left[1 + \left(\frac{B}{2Y_0}\right)^2\right]$$

or, since

$$\left(\frac{B}{Y_0}\right)^2 = \left(\frac{Z_0}{X}\right)^2,$$

$$\alpha = 10 \log\left[1 + \left(\frac{Z_0}{2X}\right)^2\right]. \qquad (34)$$

Now by (34), as long as the reactance is greater than some minimum value, the attenuation will be lower than some maximum value. From Fig. 19, this is possible from l/λ_1 to l/λ_2. If λ_1 corresponds to f_1, λ_2 corresponds to f_2, and $f_2 = Nf_1$ (where N is the bandwidth factor), then $\lambda_2 = \lambda_1/N$. To find N, set $X_1 = X_2$; then

$$N = \frac{\lambda_1}{2l} - 1. \qquad (35)$$

Combining (33)–(35) gives

$$N = \pi\left[\arctan\left(2\,\frac{Z_g}{Z_0}\,\sqrt{10^{\alpha/10} - 1}\right)^{-1}\right]^{-1} - 1. \qquad (36)$$

The equation is plotted in Fig. 20. For $Z_g/Z_0 > 5$ and $\alpha \leq 1$,

$$N \approx 3\,\frac{Z_g}{Z_0}\,\sqrt{\alpha}. \qquad (37)$$

Modifying a $Z_0 = 50$-ohm coaxial T so that one arm has a 42 AWG wire for a center conductor, a Z_g of 325 ohms is possible, which gives a $Z_g/Z_0 = 6.5$ and $N = 20$ for $\alpha = 1$ db. Thus, one biasing lead can be made to work from 4000 Mc down to 200 Mc. It is pointed out that the 1-db reflection will exist only at the upper and lower limits. Between these limits, the insertion loss of the biasing lead will be less than 0.1 db over a 6-to-1 frequency range. Knowing N, l can be found from (35). More precisely, l can be determined by using the upper frequency and (33) and (34) for a given α. If a 1-db attenuation is allowed and some other reactive element is causing 1-db insertion loss (by itself), these can at worst add up to 3.6 db as in Fig. 15. By observing tuning procedures such as the spacing in Fig. 14, the biasing lead insertion losses can cancel at a frequency. As the frequency is decreased, the spacing will cross optimum mismatch, but the insertion loss of each element will be reduced at the lower frequency.

The bandwidth attainable by using a straight center conductor is limited by the smallest diameter of wire that can be tolerated. Greater bandwidth can be attained with helical center conductor (coaxial) transmission line because of its higher characteristic im-

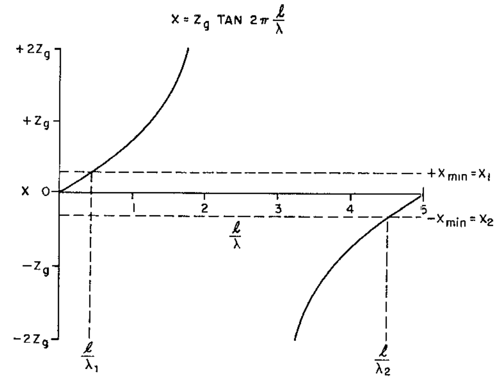

Fig. 19—Reactance of a straight biasing lead as a function of physical length, wavelength, and characteristic impedance Z_g.

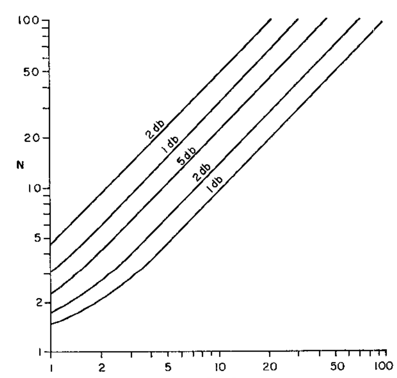

Fig. 20—Bandwidth of one biasing lead as a function of maximum insertion loss and the ratio of biasing lead characteristic impedance Z_g to main transmission line characteristic impedance Z_0.

pedance. Expressions for this type of line are derived in Appendix II, and the results are plotted in Fig. 21. From Fig. 21, it is seen that characteristic impedances on the order of 2000 ohms are easily obtained. Also from Fig. 21, a biasing lead with such a characteristic impedance, when used with a 50-ohm transmission line switch, would allow a 100-to-1 bandwidth with 0.4-db insertion loss (due to the biasing lead) at the extremes. An inductor of this type could be used profitably with the switch shown in Figs. 16 and 17.

VII. Power

It was shown that X-band diode switches could be made to isolate microwave power as high as one watt by choosing diodes having a high reverse breakdown voltage, E_b [10]. The reverse breakdown voltage, however, is not the only factor determining the maximum incident power the diode can switch; it limits only the peak power the diode can control. The diode series resistance R_s and the power the diode can dissipate $\overline{P}_d$ determine the average power the diode can switch.

As shown in Fig. 22(a), the peak RF voltage which can be applied to a diode without appreciable conduction is $E=E_b/2$. If the impedance of the series diode is high, then the maximum available peak power $\hat{P}_i$ which the switch can isolate is, approximately,

$$\hat{P}_i = \frac{E^2}{8Z_0} = \frac{E_b^2}{32Z_0} \cdot \tag{38}$$

Since the highest E_b available (in gold-bonded diodes) is about 125 volts, such a diode can isolate a peak incident power of about 10 watts in a 50-ohm transmission line, provided the power dissipated in the diode under these conditions is within the dissipation rating of the diode.

The maximum average incident power that a series diode can switch to the load is limited by the power $\overline{P}_d$ dissipated in R_s. Referring to Fig. 22(c), $P_L/P_d = Z_0/R_s$. If very little power is reflected, then

$$\overline{P}_i \approx \overline{P}_L + \overline{P}_d = \overline{P}_d\left(1 + \frac{Z_0}{R_s}\right) \approx \overline{P}_d \frac{Z_0}{R_s} \cdot \tag{39}$$

The dissipation rating of available switching diodes ranges from $0.08-0.2$ watt. For example, assuming that $\overline{P}_d = 0.1$ watt, $Z_0 = 50$ ohms, and $R_s = 5$ ohms, results in $\overline{P}_i = 1.1$ watts.

It is noted that for modulated incident power, the incident power may be greater than the maximum permissible average power provided the repetition rate of the modulation is sufficiently high to permit thermal averaging by the diode. In the event that the maximum power ratings of the diode are exceeded somewhat, the diode will not suddenly be destroyed but the switching characteristics will be temporarily degraded. In some applications, the degraded switching characteristics may still be satisfactory in which case the diode can switch larger RF incident power than indicated above.

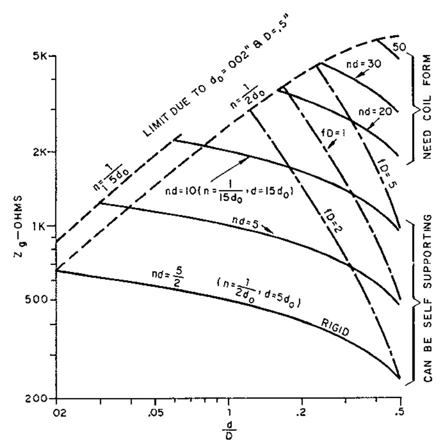

Fig. 21—Characteristic impedance of a helical center coaxial transmission line as a function of d/D, helix diameter to outer conductor diameter, from (60) for various values of nd.

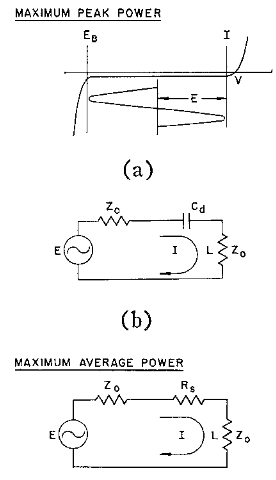

Fig. 22—Voltage-current characteristic of a diode and series equivalent circuits for determining maximum peak and average power the diode can switch.

For applications in which the diode is in the isolation state part of the time, incident CW power greater than the rated average power can be switched. The power dissipation of the diode in the isolation state (40) is usually less than in the ON state

$$\overline{P}_d \approx 4\frac{R_sZ_0}{X^2}\overline{P}_i. \tag{40}$$

The value of X is related to the isolation as indicated in Fig. 6. Higher power can be controlled by use of more than one diode.

To obtain the peak power which a shunt diode can switch, reference is made to Fig. 1, in which Y is replaced by C_d. The maximum voltage is just E, as shown in the equivalent circuit.

$$P_L = \frac{1}{2}E^2Y_0 = \frac{E_b^2}{8Z_0} \tag{41}$$

A 125-volt shunt diode in 50-ohm transmission line can switch 40 watts of incident peak power in this configuration. Higher peak power would result in increased insertion loss, and more diodes would only make the insertion loss greater.

The average power a shunting diode can isolate is determined by making Y equal to $1/R_s(=G_s)$ in Fig. 1. Then as in the case of the series diode,

$$\overline{P}_i' = \overline{P}_d'\left(\frac{Z_0}{4R_s}+1\right) \approx \frac{Z_0}{4R_s}\overline{P}_d'. \tag{42}$$

In a 50-ohm transmission line, a 5-ohm, gold-bonded diode can switch average power of about 0.3 watt in this configuration.

To determine the highest CW power that a diode can switch, the transmission line impedance is varied so that the peak power rating of the diode and average power rating of the diode are equal. Assuming for the shunt diode that

$$\hat{P}_i' = \frac{E_b^2}{8Z_0} \quad \text{and} \quad \overline{P}_i' = \overline{P}_d\frac{Z_0}{4R_s},$$

for the series diode that

$$\hat{P}_i = \frac{E_b^2}{32Z_0} \quad \text{and} \quad \overline{P}_i = P_d\frac{Z_0}{R_s},$$

and that the optimum characteristic impedance is used in each case, then the diode in both configurations can switch the same amount of CW power

$$\overline{P}_i = E_b\sqrt{\frac{\overline{P}_d}{32R_s}}\,.$$

A 5-ohm, 125-volt, gold-bonded diode can switch 2.8 watts CW power in a 180-ohm transmission line.

VIII. Further Techniques

A. Alternate Switch Configuration

Another technique of switching warrants mention. If the diode terminates a quarter-wavelength arm of a T, the whisker can be made part of the length of line; and the contact impedance Z_c is transformed by virtue of the transforming action of a quarter-wavelength line section to an admittance

$$\frac{Y}{Y_0} = Z_c\left(\frac{Z_0}{Z_{0,\lambda/4}^2}\right),$$

in which $Z_{0,\lambda/4}$ and Z_0 are characteristic impedances, respectively, of the quarter-wavelength section and the main transmission line. This configuration is illustrated in Fig. 23. If $Z_{0,\lambda/4}=Z_0$, the series diode impedance of Fig. 6 dictates the switching behavior in spite of the configuration being in shunt with the main guide. Also,

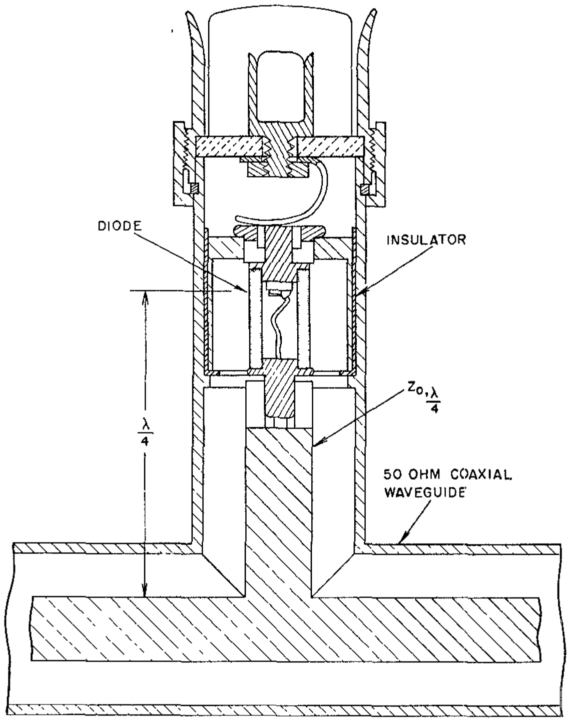

Fig. 23—Phantom view of a diode in a quarter wavelength T arm.

the diode contact impedance rather than the entire diode impedance describes the switching since the cartridge is part of the $\lambda/4$ configuration. Using a 1N263, greater than 20-db isolation has been attained over a 5 per cent bandwidth at 1 Gc, with an associated 1 db insertion loss. Isolation greater than 10 db was available over a 20 per cent bandwidth with little change from 1 db in insertion loss.

B. Switching Speed

It has been found that a germanium point-contact diode causing switching in X-band waveguide can provide about half of maximum isolation in about 0.2×10^{-9} second. Later observations indicate the diode provides full isolation in about 20×10^{-9} second. Varactors and gold-bonded diodes may differ from these point-contact diodes if forward conduction is used for part of the switching. The makers of gold-bonded diodes claim switching times of about 0.5 μsec. If germanium point-contact diodes are used in a switch, or these other diodes are found to be faster, the biasing lead inductance must be small to avoid increasing the switching time or decreasing the maximum modulation rate. To attain this the bandwidth of the biasing leads is made no larger than it has to be, using the lowest possible characteristic impedance. It is noted that similar precautions should be taken with the detector.

RF leakage out the biasing network (Fig. 18) will be small by virtue of the network needed to prevent interaction between the RF and bias circuits for optimum switching. If high-speed switching is not needed, C_1 can be increased and additional inductance can be placed in series with V to provide any desired broad-band RF leakage suppression.

C. *Whisker Inductance*, L_w

In addition to the technique mentioned in Section III, another suggested method of reducing the effect of L_w is to actually reduce L_w by surrounding the wire whisker with soft, high-conductivity rubber epoxy as shown in Fig. 24. The soft rubber would allow the whisker to flex for thermal variations of the cartridge and yet provide low inductance. The whisker could be encapsulated by drilling a hole in the cartridge near the base of the whisker and forcing the required amount of uncured epoxy into the cartridge. With the above technique for reducing L_w, it should be possible to make Mode 1 switches operable up to 10 Gc.

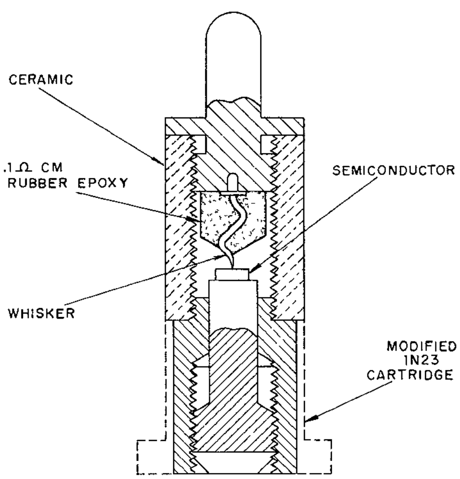

Fig. 24—Phantom view of a diode filled with conducting rubber epoxy for the purpose of reducing L_w.

IX. Conclusions

Comparison of the series and shunt connected diodes reveals that the best whisker-type diodes, when used in series configuration, provide higher isolation and wider bandwidth over that of the shunt configuration by a factor of 4. It is anticipated that pill-type diodes with low R_s will allow competitive isolation and bandwidth in the shunt configuration.

It is concluded that Mode 1 operation with multiple diodes affords the greatest bandwidth. The addition of L_T in parallel with C_c+C_d moves Mode 1 to a higher frequency. Mode 2 is useful at even higher frequencies. Mode 3 is useful at the highest frequencies, but adding the series inductor to reduce the insertion loss provides a narrow-band insertion loss (approximately that which would result from the total inductance) and reduces the bandwidth of the isolation. Most efficient low-power switching is obtained with the resonant shunt mode.

Broad-band biasing is obtained by using helical center conductor coaxial transmission lines, which are equally useful in detectors, coaxial transistors, and (in eliminating lower frequencies) as a form of high-pass filter.

In addition to using the single-pole, single-throw basic switching configurations as switches, they may be utilized as the basic element for making attenuators, multipole switches [5], phase modulators, and frequency translators [11]. Present diodes can switch incident peak power of 10 watts and incident average power of 1 watt.

Appendix I

Multiple-Element Spacing and Isolation

One shunt susceptance element with a matched load behind it results in a normalized admittance of

$$\frac{Y}{Y_0} = 1 + j\frac{B}{Y_0}\cdot$$

This can be matched out (or compensated) by placing a second equal shunt susceptance a distance l toward the generator, which would render the first admittance

$$\frac{Y}{Y_0} = 1 - j\frac{B}{Y_0}\cdot$$

This distance is [9]

$$l = \frac{\lambda_g}{2\pi}\tan^{-1}\frac{2}{B/Y_0}\cdot \tag{43}$$

Similarly, for one series reactive element,

$$\frac{Z}{Z_0} = 1 + j\frac{X}{Z_0}$$

is transformed to

$$\frac{Z}{Z_0} = 1 - j\frac{X}{Z_0}$$

by a displacement of

$$l = \frac{\lambda_g}{2\pi}\tan^{-1}\frac{2}{X/Z_0}\cdot \tag{44}$$

A second equal reactive element, spaced a distance l from the first, would result in minimum insertion loss, or match. Eqs. (43) and (44) are plotted in Fig. 14, as the curve for match. For maximum attenuation, the second equal reactive element is placed where the impedance of the first is transformed to

$$\frac{1}{1 - j\dfrac{X}{Z_0}}$$

which is

$$l = \frac{\lambda_g}{2\pi}\left(\tan^{-1}\frac{2}{X/Z_0}\right) + \frac{\lambda_g}{4}\cdot \tag{45}$$

This is plotted in Fig. 14 as the curve for mismatch.

Power loss due to reflection [12] is

$$\alpha = 10\log\frac{\left(\frac{R}{Z_0}+1\right)^2+\left(\frac{X}{Z_0}\right)^2}{4\left(\frac{R}{Z_0}\right)}. \quad (46)$$

One series reactive element gives

$$\frac{Z}{Z_0} = 1 + j\left(\frac{X}{Z_0}\right),$$

$$\alpha_1 = 10\log\left[\frac{4+\left(\frac{X}{Z_0}\right)^2}{4}\right] \quad (47)$$

and

$$\left(\frac{X}{Z_0}\right)^2 = 4(10^{\alpha_1/10}-1). \quad (48)$$

Two series reactive elements optimumly spaced give

$$\frac{Z}{Z_0} = \frac{1}{1-j\left(\frac{X}{Z_0}\right)} + j\left(\frac{X}{Z_0}\right)$$

or

$$\frac{Z}{Z_0} = \frac{1+j\left(\frac{X}{Z_0}\right)\left[2+\left(\frac{X}{Z_0}\right)^2\right]}{1+\left(\frac{X}{Z_0}\right)^2}. \quad (49)$$

Then,

$$\alpha_2 = 10\log\left[\frac{\left\{\frac{1}{1+\left(\frac{X}{Z_0}\right)^2}+1\right\}^2+\left\{\frac{\frac{X}{Z_0}\left(2+\frac{X^2}{Z_0^2}\right)}{1+\left(\frac{X}{Z_0}\right)^2}\right\}^2}{4\frac{1}{1+\left(\frac{X}{Z_0}\right)^2}}\right]$$

or

$$\alpha_2 = 20\log\frac{2+\left(\frac{X}{Z_0}\right)^2}{2}, \quad (50)$$

$$\alpha_{x2} = \alpha_2 - 2\alpha_1$$

$$= 20\log\left[\frac{2+\left(\frac{X}{Z_0}\right)^2}{2}\right] - 20\log\left[\frac{4+\left(\frac{X}{Z_0}\right)^2}{4}\right]$$

or

$$\alpha_{x2} = 20\log\left[\frac{4+2\left(\frac{X}{Z_0}\right)^2}{4+\left(\frac{X}{Z_0}\right)^2}\right] = 20\log\left[2-10^{-\alpha_1/10}\right]. \quad (51)$$

For $\alpha_1 \geq 20$ db, $\alpha_{x2} = 6$ db.

For $\alpha_1 \leq 0.5$ db, $\alpha_{x2} \approx 2\alpha_1$.

For the maximum α from 2 or more, N_d, small shunt susceptances

$$Y_2 = \frac{1}{1-j\left(\frac{B}{Y_0}\right)} + j\left(\frac{B}{Y_0}\right) \approx 1 + j2\left(\frac{B}{Y_0}\right)$$

$$Y_{N_d} = 1 + jN_d\left(\frac{B}{Y_0}\right) \quad (52)$$

$$\alpha = 10\log\frac{\left(\frac{G}{G_0}+1\right)^2+\left(\frac{B}{Y_0}\right)^2}{4\left(\frac{G}{Y_0}\right)}$$

$$= 10\log\left\{1+\frac{N_d^2\frac{B^2}{Y_0^2}}{4}\right\}. \quad (53)$$

Log $(1+\delta) = 0.435\delta$ for $\delta \leq 0.1$. So,

$$\alpha = \frac{4.35}{4}N_d^2\frac{B^2}{Y_0^2} \quad \text{for } N_d^2\frac{B^2}{Y_0^2} \leq 0.5. \quad (54)$$

The calculation for the extra attenuation resulting from the third, or higher, additional identical optimum-spaced elements is simplified by the fact that the addition of equal reactance (or susceptance) results in a total impedance (or admittance) which has repeatedly the same reflection coefficient angle, and that the corresponding reciprocal of the complex conjugate of the impedance has another repeating reflection coefficient angle. Thus, the total impedance (or admittance) for one more element can be found by taking the reciprocal of the complex conjugate of the total impedance (or admittance) from the addition of the last element and then adding the new element. The extra attenuation for the second, third, and fourth additional elements as well as the limit for large numbers of elements is plotted in Fig. 15. The total attenuation α_T from N elements is

$$\alpha_T = N\alpha_1 + \sum_{n=2}^{N}\alpha_{xn}. \quad (55)$$

Appendix II

Helical Center Conductor [13]

When a helix of average diameter d (inches), n turns per inch, wire diameter d_0 (inches), and length l (inches) is centered coaxially in a hollow cylinder of inside diameter D (inches), the inductance in microhenries per axial foot is

$$L \approx 0.30n^2d^2[1 - (d/D)^2] \tag{56}$$

and the capacitance in picofarads per axial foot is

$$C \approx \frac{7.4\epsilon}{\log_{10}(D/d)}, \tag{57}$$

where ϵ is the relative dielectric constant of the material separating the helix and the outer conductor. In the present application, the dielectric is air, for which ϵ is unity. Eqs. (56) and (57) are most accurate when

$$1.0 \leq l/D < 4.0$$

$$0.45 < d/D < 0.6$$

and

$$n \approx \frac{1}{2d_0},$$

but they can be used as an approximate guide outside these limits.

The characteristic impedance of this line is

$$Z_0 = \sqrt{\frac{L}{C}} \times 10^3 \cdot \tag{58}$$

and the propagation constant is

$$T = \sqrt{LC} \times 10^{-9}. \tag{59}$$

Substituting (56) and (57) in (58) and (59), Z_0 and T are, respectively,

$$Z_0 = 202nd\sqrt{[1 - (d/D)^2] \log (D/d)} \tag{60}$$

$$T = 1.49nd\sqrt{\frac{1 - (d/D)^2}{\log (D/d)}} \times 10^{-9}. \tag{61}$$

Eq. (60) is plotted in Fig. 21 for various values of nd. The limits imposed by $d_0 = 0.002$ inch and $D = 0.5$ inch for

$$n = \frac{1}{2d_0} \quad \text{and} \quad n = \frac{1}{1.5d_0}$$

are shown as the dashed curves. For larger d_0 or smaller D this limit is lower. Another limit is imposed by the requirement that $l/d > 1.0$.

It is desired that the line be $\frac{1}{2}$ wavelength long electrically at some frequency slightly higher than f_2 (Fig. 19). The electrical length K in wavelengths at the frequency f in gigacycles is defined as

$$K = \frac{fTl}{12} \times 10^9. \tag{62}$$

Assuming $l/d = 1$ and $K = \frac{1}{2}$ and solving (60) by substituting (61) and (62) in it, the following limit is placed on Z_0:

$$Z_0 = \left[\frac{(202)(12)(10^9)\sqrt{[1 - (d/D)^2] \log (D/d)}}{(1.49)(2)(10^9)fd}\right] \cdot \left[\sqrt{\frac{\log (D/d)}{1 - (d/D)^2}}\right] = \frac{813}{fD}\left(\frac{D}{d}\right) \log \left(\frac{D}{d}\right) \cdot \tag{63}$$

Eq. (63) is plotted for various values of fD as the dot-dash curves in Fig. 21. Above each curve l/d is less than 1.0, which is undesirable. If D is 0.5 inch and f is 4 Gc, then the highest possible characteristic impedance is 3000 ohms. d/D is outside of the desirable limits; but coils fabricated and tested with $d/D \approx 0.2$ demonstrate higher impedance and resonate at 5 per cent to 10 per cent higher frequency than predicted, which provides a margin of safety.

X. Acknowledgment

The author would like to express his appreciation to B. Haimowitz and L. Riebman of American Electronic Laboratories, Inc. for helpful discussions and for supplying several Mode 1½ switches.

Bibliography

[1] M. A. Armistead, E. G. Spencer and R. D. Hatcher, "Microwave semi-conductor switch," Proc. IRE, vol. 44, p. 1875; December, 1956.

[2] R. V. Garver, J. A. Rosado and E. F. Turner, "Theory of the germanium diode microwave switch," IRE Trans. on Microwave Theory and Techniques, vol. MTT-8, pp. 108–111; January, 1960.

[3] L. Riebman, "Study of Wide-Open Receiver Detection Capabilities Interim Report," American Electronic Labs., Inc., Philadelphia, Pa., AEL Tech. Rept. 57052-3, Signal Corps Contract DA-36-039-sc-74813; July–December, 1958.

[4] L. Riebman, "Study of Wide-Open Receiver Detection Capabilities Final Progress Report," American Electronic Labs., Inc., Philadelphia, Pa., AEL Tech. Rept. 57052-F, Signal Corps Contract DA-36-039-sc-74813; October–June, 1959.

[5] M. Bloom, "Single-Pole Double-Throw Wideband Microwave Switch," presented at the PGMTT Natl. Symp., Harvard University, Cambridge, Mass.; June 2, 1959.

[6] R. V. Garver and J. A. Rosado, "Microwave diode cartridge impedance," IRE Trans. on Microwave Theory and Techniques, vol. MTT-8, pp. 104–107; January, 1960.

[7] R. V. Garver, E. G. Spencer and M. A. Harper, "Microwave semi-conductor switching techniques," IRE Trans. on Microwave Theory and Techniques, vol. MTT-6, pp. 378–383; October, 1958.

[8] R. V. Garver, "High-speed microwave switching of semiconductors—II," IRE Trans. on Microwave Theory and Techniques, vol. MTT-7, pp. 272–276; April, 1959.

[9] G. C. Southworth, "Principles and Applications of Waveguide Transmission," D. Van Nostrand Co., Inc., New York, N. Y., p. 220; 1950.

[10] R. V. Garver, E. G. Spencer and R. C. LeCraw, "High-speed microwave switching of semiconductors," *J. Appl. Phys.*, vol. 28, pp. 1336–1338; November, 1957.

[11] E. M. Rutz and J. E. Dye, "Frequency Translation by Phase Modulation," 1957 IRE Wescon Convention Record, pt. 1, pp. 201–207.

[12] T. Moreno, "Microwave Transmission Design Data," Sperry Gyroscope Co., Inc., Great Neck, N. Y., p. 22; 1944.

[13] H. P. Westman, "Reference Data for Radio Engineers," IT&T, New York, N. Y., 4th ed., p. 600; 1956.